

SUPPORTING INFORMATION

Towards Interpretation of Intermolecular Paramagnetic Relaxation Enhancement Outside the Fast Exchange Limit

Alberto Ceccon, G. Marius Clore*, and Vitali Tugarinov*

Laboratory of Chemical Physics, National Institute of Diabetes and Digestive and Kidney
Diseases, National Institutes of Health, Bethesda, Maryland 20892-0520

Analytical solution for lifetime line broadening (ΔR_2).

The coupled evolution of magnetization of a system undergoing two-site exchange between the free state of a protein (observable state A) and its bound state ('dark' state B) in the absence of chemical shift differences between these two states, can be expressed through a set of simplified Bloch-McConnell equations (Helgstrand, M. et al. 2000; McConnell H.M. 1958),

$$\frac{d}{dt} \begin{bmatrix} I^A \\ I^B \end{bmatrix} = - \begin{bmatrix} R_2^A + k_{\text{on}}^{\text{app}} & -k_{\text{off}} \\ -k_{\text{on}}^{\text{app}} & R_2^B + k_{\text{off}} \end{bmatrix} \begin{bmatrix} I^A \\ I^B \end{bmatrix} \quad (\text{S1})$$

where I^A and I^B are the transverse magnetizations of states A and B, respectively, $k_{\text{on}}^{\text{app}}$ is the apparent association rate constant, k_{off} is the dissociation rate constant, and R_2^A and R_2^B are the respective intrinsic transverse relaxation rates of the two states in the absence of exchange. Lifetime line broadening (ΔR_2) of the observable resonances of a protein in the presence of much larger particles to which the protein can bind, can be calculated from the solution of Eq. S1 for I^A as described in detail in our previous

publications (Libich et al. 2015; Libich et al. 2013). The system of differential equations in Eq. S1 has closed-form analytical solutions: for initial conditions $\{I^A(0) = p_A; I^B(0) = 0\}$, where p_A is the equilibrium population of state A ($p_A = k_{\text{off}} / k_{\text{ex}}$, where $k_{\text{ex}} = k_{\text{on}}^{\text{app}} + k_{\text{off}}$) the time evolution of I^A can be expressed as the weighted sum of two exponential terms:

$$I^A(t) = A_+ e^{-(R_2^A + R_2^B + k_{\text{off}} + k_{\text{on}}^{\text{app}} - 2\eta)t/2} + A_- e^{-(R_2^A + R_2^B + k_{\text{off}} + k_{\text{on}}^{\text{app}} + 2\eta)t/2} \quad (\text{S2})$$

where

$$\eta = (1/2)[(R_2^B - R_2^A)^2 + (k_{\text{off}} + k_{\text{on}}^{\text{app}})^2 + 2(R_2^B - R_2^A)(k_{\text{off}} - k_{\text{on}}^{\text{app}})]^{1/2} \quad (\text{S3})$$

and $A_{\pm} = (p_A / 2)[1 \pm (R_2^B - R_2^A + k_{\text{off}} - k_{\text{on}}^{\text{app}}) / 2\eta]$. When the differences between the transverse relaxation rates R_2^A and R_2^B are large, and exchange is fast on the relaxation time-scale ($k_{\text{ex}} > R_2^B - R_2^A$) as is the case in the present study, the second term in Eq. S2 decays much more rapidly than the first, and can therefore, for all practical purposes, be neglected. Under these conditions, the observed rate of decay of I^A is, to a very good approximation, equal to $R_{2,\text{obs}}^A = (R_2^A + R_2^B + k_{\text{off}} + k_{\text{on}}^{\text{app}} - 2\eta) / 2$, and

$$\Delta R_2 = R_{2,\text{obs}}^A - R_2^A = (R_2^B - R_2^A + k_{\text{off}} + k_{\text{on}}^{\text{app}} - 2\eta) / 2 \quad (\text{S4})$$

Note that in the limit of very high R_2^B values (*i.e.* when exchange is slow on the transverse relaxation time-scale, $R_2^B \gg k_{\text{ex}}$) the expression in Eq. S4 asymptotically approaches the value of $k_{\text{on}}^{\text{app}}$ ($\lim_{R_2^B \rightarrow \infty} \Delta R_2 = k_{\text{on}}^{\text{app}}$), while in the limit of fast exchange ($k_{\text{ex}} \gg R_2^B - R_2^A$), ΔR_2 approaches $p_B(R_2^B - R_2^A) \approx p_B R_2^B$, where p_B is the population of the bound state B ($p_B = 1 - p_A = k_{\text{on}}^{\text{app}} / k_{\text{ex}}$).

Preparation of NMR samples.

Recombinant ubiquitin was expressed and purified as described previously (Varadan et al. 2004). Ubiquitin samples were uniformly ^{15}N -labeled and deuterated (U- $[\text{H}/^{15}\text{N}]$) and selectively $^{13}\text{CH}_3$ -labeled at Ile δ 1, Val γ and Leu δ positions: [Ile δ 1- $^{13}\text{CH}_3$ /Leu, Val- $^{13}\text{CH}_3$ / $^{12}\text{CD}_3$]. Of note, only one of the two methyl groups of the isopropyl moieties of Val and Leu is ^{13}C -labeled and protonated (Tugarinov and Kay 2004; Tugarinov et al. 2006). All NMR samples were prepared in 10 mM phosphate buffer ($\text{K}_2\text{HPO}_4/\text{KH}_2\text{PO}_4$),

pH 6.8, and 7% D₂O/93% H₂O. The final concentration of ubiquitin was 0.6 mM and in all experiments was kept constant upon addition of the liposome solution (see below).

Preparation and characterization of liposome solutions.

The sodium salt of 1-palmitoyl-2-oleoyl-*sn*-glycero-3-phospho-(1'-*rac*-glycerol) (POPG), 1-palmitoyl-2-oleoyl-*sn*-glycero-3-phosphocholine (POPC), and the gadolinium salt of 1,2-distearoyl-*sn*-glycero-3-phosphoethanolamine-N-diethylenetriaminepentaacetic acid (18:0 PE-DTPA-Gd³⁺) were purchased from Avanti Polar Lipids (Alabaster, AL). Diamagnetic liposomes were prepared by dissolving an aliquot of POPG or POPC phospholipids with 20 % (mol/mol) cholesterol in chloroform to ensure a clear homogeneous solution. For preparation of the paramagnetic liposomes, 10 % (mol/mol) of 18:0 PE-DTPA-Gd³⁺ phospholipid was added to the lipid mixture. The solvent was then removed and the lipid suspension dried as a thin film in a round-bottom glass flask by slow evaporation under nitrogen flux. The film was then dispersed by gentle mixing in 10 mM phosphate buffer (K₂HPO₄/KH₂PO₄), pH 6.8, to a final lipid stock concentration of 10 mM. After addition of the hydrating medium, the lipid suspension was maintained above the transition temperature ($T_m = -2$ °C) for 12 hrs.

Small unilamellar vesicles (SUV) were prepared via probe tip sonication (Misonix, NY) without cooling at 15 Watts for 20 min. After sonication, SUV solutions were centrifuged to sediment small bits of metal released by the sonication tip.

Homogenous large unilamellar vesicles (LUV) were formed by pressure extrusion using an Avanti Polar device. Repeated extrusions of the lipid suspension were performed through polycarbonate filters (1 μm, 400 nm, 100 nm) to obtain uniformly sized unilamellar vesicles of ~100 nm in diameter. The liposome solutions were stored in the dark at room temperature to prevent lipid oxidation. The polydispersity of the liposome solutions was characterized by dynamic light scattering with a Zetasizer Nano ZS instrument (Malvern Instruments, USA) operating at a wavelength of 633 nm at 25°C. Samples were loaded into disposable cells and diluted to 0.5 mM with phosphate buffer pH 6.8.

NMR spectroscopy.

All NMR experiments were recorded at 25 °C using Bruker Avance-III spectrometers, equipped with Bruker TCI triple resonance *z*-axis gradient cryogenic probes, at proton Larmor frequencies of 700.24 and 500.68 MHz. All experiments were performed on a 0.6 mM sample of [²H/¹⁵N/Ileδ₁-¹³CH₃/Leu,Val-¹³CH₃/¹²CD₃]-labeled ubiquitin dissolved in 10 mM phosphate buffer (pH 6.8), 7% D₂O/93% H₂O (v/v). All NMR measurements were performed in the absence and presence of diamagnetic or paramagnetic negatively charged POPG vesicles with a protein/lipid ratio (mol/mol) of 1:2 for LUVs and 1:0.5 for

SUVs. Control experiments were performed on ubiquitin with zwitterionic POPC LUV liposomes and on 0.5 mM [$^2\text{H}/^{15}\text{N}/^{13}\text{CH}_3/\text{Leu,Val-}^{13}\text{CH}_3/^{12}\text{CD}_3$]-labeled GB1 in the presence of negatively charged POPG LUV vesicles keeping the same protein:lipid ratio as specified above.

$^1\text{H}_\text{N}$, $^1\text{H}_\text{methyl}$ and $^{13}\text{C}_\text{methyl}$ spin relaxation rate measurements.

Free-precession $^1\text{H}_\text{N}$ - R_2 and $^1\text{H}_\text{methyl}$ - R_2 relaxation rates of ubiquitin were measured as described earlier (Ceccon et al. 2016). $^{13}\text{C}_\text{methyl}$ - R_2 values in the presence of diamagnetic (R_2^{dia}) and paramagnetic (R_2^{para}) vesicles were extracted from the measured $R_{1\rho}$ and R_1 rates using the following relationship:

$$R_2 = (R_{1\rho} - R_1 \cos^2\theta)/\sin^2\theta \quad (\text{S5})$$

where θ is the angle subtended by the effective spin-lock field with respect to the external magnetic field (90° is on-resonance with the spin-lock field). $^{13}\text{C}_\text{methyl}$ $R_{1\rho}$ and R_1 measurements were performed using the pulse schemes described previously (Fawzi et al. 2014). A spin-lock field strength of 1.6 kHz was employed to suppress chemical exchange (R_{ex}) contributions to $^{13}\text{C}_\text{methyl}$ relaxation rates. $^{13}\text{C}_\text{methyl}$ - $R_{1\rho}$ spectra were recorded with spin-lock periods of 40, 60, 80, 100, 120, 140, 160 and 200 ms, while $^{13}\text{C}_\text{methyl}$ - R_1 measurements were performed using delays of 40, 120, 200, 500 and 600 ms. The same spin-lock field strengths but with shorter spin-lock periods was used for $R_{1\rho}$ measurements in the presence of paramagnetic vesicles: 20, 40, 60, 80, 100, 120, 140 and 160 ms.

Relaxation delays of 20, 40, 80, 100, 120 and 160 ms were used for measuring free-precession $^1\text{H}_\text{methyl}$ - R_2 relaxation rates on GB1 with diamagnetic vesicles, while delays of 20, 28, 34, 40, 48 and 60 ms were used in presence of paramagnetic vesicles. $^{13}\text{C}_\text{methyl}$ - $R_{1\rho}$ spectra were recorded with spin-lock periods of 40, 80, 120, 160, 200 and 240 ms, while $^{13}\text{C}_\text{methyl}$ - R_1 measurements were performed using the relaxation delays of 40, 120, 200, 500 and 600 ms.

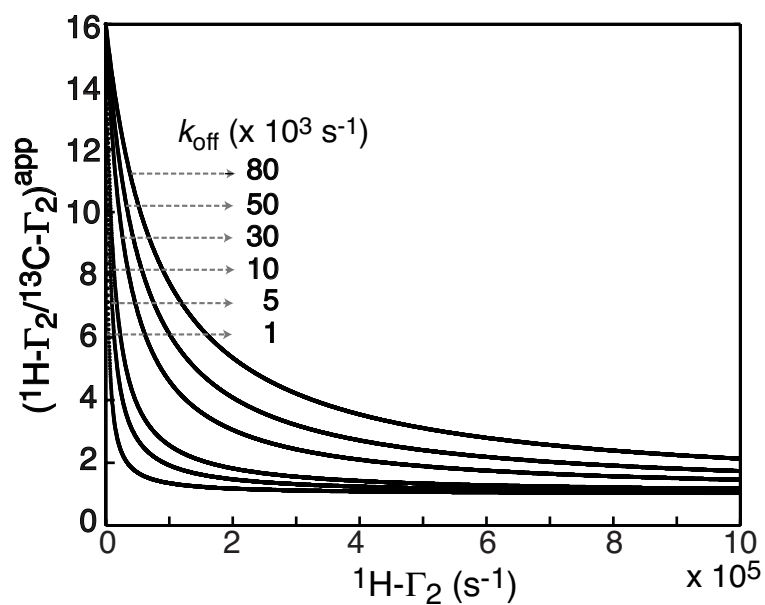


Figure S1. Theoretical dependence of the $(^1\text{H}\text{-}\Gamma_2/^{13}\text{C}\text{-}\Gamma_2)^{\text{app}}$ ratio on the ‘true’ $^1\text{H}\text{-}\Gamma_2$ rate for different values of the dissociation rate constant k_{off} . Curves are calculated by solving Eq. 1 of the main text numerically using the same parameters of the ubiquitin-LUV liposome system given in Figure 1 of the main text except that k_{off} is varies from 1000 to 80,000 s^{-1} : $k_{\text{on}}^{\text{app}} = 50 \text{ s}^{-1}$; $R_2^{\text{A}} = 10 \text{ s}^{-1}$; $R_2^{\text{B}} = 13,500 \text{ s}^{-1}$.

Supplementary references

- Ceccon, A., Tugarinov, V., Bax, A. & Clore, G. M. Global Dynamics and Exchange Kinetics of a Protein on the Surface of Nanoparticles Revealed by Relaxation-Based Solution NMR Spectroscopy. *J. Am. Chem. Soc.* **138**, 5789–5792 (2016).
- Fawzi, N. L., Ying, J., Torchia, D. A. & Clore, G. M. Kinetics of amyloid beta monomer-to-oligomer exchange by NMR relaxation. *J. Am. Chem. Soc.* **132**, 9948–9951 (2010).
- Fawzi, N. L., Libich, D. S., Ying, J., Tugarinov, V. & Clore, G. M. Characterizing methyl-bearing side chain contacts and dynamics mediating amyloid β protofibril interactions using ^{13}C (methyl)-DEST and lifetime line broadening. *Angew. Chem. Int. Ed. Engl.* **53**, 10345–10349 (2014).
- Helgstrand, M., Hård, T. & Allard, P. Simulations of NMR pulse sequences during equilibrium and non-equilibrium chemical exchange. *J. Biomol. NMR* **18**, 49–63 (2000).
- Libich, D. S., Tugarinov, V. & Clore, G. M. Intrinsic unfoldase/foldase activity of the chaperonin GroEL directly demonstrated using multinuclear relaxation-based NMR. *Proc. Natl. Acad. Sci. U.S.A.* **112**, 8817–8823 (2015).
- Libich, D. S., Fawzi, N. L., Ying, J. & Clore, G. M. Probing the transient dark state of substrate binding to GroEL by relaxation-based solution NMR. *Proc. Natl. Acad. Sci. U.S.A.* **110**, 11361–11366 (2013).
- McConnell, H. M. Reaction rates by nuclear magnetic resonance. *J. Chem. Phys.* **28**, 430–431 (1958).
- Tugarinov, V. & Kay, L. E. An isotope labeling strategy for methyl TROSY spectroscopy. *J. Biomol. NMR* **28**, 165–172 (2004).
- Tugarinov, V., Kanelis, V. & Kay, L. E. Isotope labeling strategies for the study of high-molecular-weight proteins by solution NMR spectroscopy. *Nature Protocols* **1**, 749–754 (2006).
- Varadan, R. *et al.* Solution conformation of Lys63-linked di-ubiquitin chain provides clues to functional diversity of polyubiquitin signaling. *J. Biol. Chem.* **279**, 7055–7063 (2004).